

## Probing equilibration with respect to isospin degree of freedom in intermediate energy heavy ion collisions

Qingfeng Li<sup>1</sup> and Zhuxia Li<sup>1,2,3</sup>

<sup>1</sup>*China Institute of Atomic Energy, P.O. Box 275 (18), Beijing 102413, People's Republic of China*

<sup>2</sup>*Center of Theoretical Nuclear Physics, National Laboratory of Lanzhou Heavy Ion Accelerator, Lanzhou 730000, People's Republic of China*

<sup>3</sup>*Institute of Theoretical Physics, Academia Sinica, P.O. Box 2735, Beijing 100080, People's Republic of China*

(Received 13 May 2001; published 21 November 2001)

We have studied equilibration with respect to isospin degree of freedom in four 96 mass systems  $^{96}\text{Ru} + ^{96}\text{Ru}$ ,  $^{96}\text{Ru} + ^{96}\text{Zr}$ ,  $^{96}\text{Zr} + ^{96}\text{Ru}$ , and  $^{96}\text{Zr} + ^{96}\text{Zr}$  at 100A MeV and 400A MeV with isospin-dependent quantum molecular dynamics. We propose that the neutron-proton differential rapidity distribution is a sensitive probe to the degree of equilibration with respect to the isospin degree of freedom. By analyzing the average  $N/Z$  ratio of emitted nucleons, light charged particles, and intermediate mass fragments (IMF), it is found that there exist memory effect in multifragmentation process. The average  $N/Z$  ratio of IMF reduces largely as beam energy increases from 100A MeV to 400A MeV that may result from the change of the behavior of the isotope distribution of IMF charges. The isotope distribution of IMF charges does also show certain memory effect at 100A MeV case but not at 400A MeV case.

DOI: 10.1103/PhysRevC.64.064612

PACS number(s): 25.70.Pq, 24.10.-i

The study of whether the equilibrium is reached or not is a prerequisite for the extraction of valid information about the thermodynamical properties of the excited system produced in the reaction. This problem has been studied theoretically and experimentally for many years. But, still there are many new problems that need to be further studied. Especially the interest is about the nature of the multifragmentation, that is, if the multifragmentation is a statistical emission process or the dynamical one [1–5]. To clarify this problem, the FOPI Collaboration recently performed a so-called “mixing experiment” using four mass 96+96 systems Ru+Ru, Zr+Zr, Ru+Zr, and Zr+Ru at 400A MeV [6,7]. To quantify conveniently the “degree of mixing,” they defined a normalized proton counting by the value of Zr+Zr and Ru+Ru

$$R_Z = \frac{2 \times Z - Z^{\text{Zr}} - Z^{\text{Ru}}}{Z^{\text{Zr}} - Z^{\text{Ru}}}. \quad (1)$$

They first measured the proton counting number for Ru+Ru and Zr+Zr, then they measured  $R_Z$  for asymmetric reaction Zr+Ru. The results of  $R_Z$  for reaction Zr+Ru showed that the protons were not emitted from an equilibrium source and the reaction was half transparent [6]. These experimental results told us that the equilibrium was not eventually reached in the reaction. However, this beautiful experimental study has only shown that at beam energy 400A MeV, the protons are emitted by a nonequilibrium source but still it cannot answer if multifragmentation is a statistical emission process or dynamical emission one at lower energy.

The aim of this work is to test the nonequilibrium effect by means of isospin degree of freedom and relevant probes stimulated by the “mixing experiments” performed by FOPI Collaboration. We will first introduce our model briefly then we study the normalized proton counting  $R_Z$  and other probes such as the proton rapidity distribution, neutron-

proton differential rapidity distribution, and the isospin distribution of emitted nucleons, light charged particles (LCP), and intermediate mass fragments (IMF), in the same collision systems at 400A MeV as well as 100A MeV. And finally a short conclusion will be given.

The isospin-dependent quantum molecular dynamics (QMD) model [4,8,9] is used in the calculations. The following modifications in QMD model are introduced. First, the isospin-dependent part of the nuclear potential is taken into account in addition to the Coulomb interaction. The symmetry potential energy per nucleon takes the following form:

$$V_{sym}(\rho, \delta) = \frac{C_S}{2} \left( \frac{\rho}{\rho_0} \right) \delta^2, \quad (2)$$

where

$$\delta = \frac{\rho_n - \rho_p}{\rho_n + \rho_p}, \quad (3)$$

and  $C_S$  is the symmetry potential strength. In this work, it is taken to be 35 MeV and the corresponding symmetry energy is about 29 MeV. Second, the isospin-dependent binary elastic scattering cross section is used. It is well known that up to hundreds of MeV, the free elastic proton-neutron cross section is about 2–3 times larger than that of proton-proton (neutron-neutron). Finally, in the treatment of the Pauli blocking, we first distinguish protons and neutrons and then we use the following two criteria:

$$\frac{4\pi}{3} r_{ij}^3 \frac{4\pi}{3} p_{ij}^3 \geq \frac{\hbar^3}{4} \quad (4)$$

and

$$P_{block} = 1 - (1 - f_i)(1 - f_j), \quad (5)$$

TABLE I. Parameters used in calculations.

| $\alpha$<br>(MeV) | $\beta$<br>(MeV) | $\gamma$ | $\rho_0$<br>(fm <sup>-3</sup> ) | K<br>(MeV) | L<br>(fm) | $C_{Yuk}$<br>(MeV) |
|-------------------|------------------|----------|---------------------------------|------------|-----------|--------------------|
| -356              | 303              | 70/60    | 0.168                           | 200        | 2.1       | -5.5               |

where  $f_i$  is the distribution function in phase space for particle  $i$  and reads as

$$f_i(\vec{r}, \vec{p}, t) = \frac{1}{\pi \hbar^3} \exp\{-[\vec{r} - \vec{r}_i(t)]^2 / 2L^2\} \times \exp\{-[\vec{p} - \vec{p}_i(t)]^2 2L^2 / \hbar^2\}, \quad (6)$$

where  $L$  is a parameter that represents the spatial spread of wave packet,  $\vec{r}_i(t)$  and  $\vec{p}_i(t)$  denote the center of the wave packet in coordinate and momentum space, respectively. The first condition gives the criterion for the uncertainty relation of the centroids of Gaussian wave packets of two particles. The second one is the probability of the Pauli blocking effect for the scattering of two particles, which is especially useful for collisions of heavy nuclei. The soft equation of state (EOS) ( $K=200$  MeV) is used in the calculations, the corresponding main parameters are listed in Table I. The secondary deexcitation on primary hot fragments is not taken into account in the present calculations. It should not change the general conclusion of this work.

We first investigate the proton counting for the mixing reactions of four mass 96+96 systems Ru+Ru, Zr+Zr, Ru+Zr, and Zr+Ru as the same as in the experimental study in Ref. [6]. According to the definition of  $R_Z$ ,  $R_Z=1$  for Zr+Zr,  $R_Z=-1$  for Ru+Ru. For asymmetric reactions Ru+Zr and Zr+Ru, it may be more convenient to express  $R_Z$  as  $R_Z=2R_{mix}-1$ , for Zr+Ru and  $R_Z=1-2R_{mix}$  for Ru+Zr, which can be derived from definition (1). Here  $R_{mix}$  is the percentage of the number of protons emitted from projectile.  $R_{mix}$  is proportional to the degree of mixing of projectile and

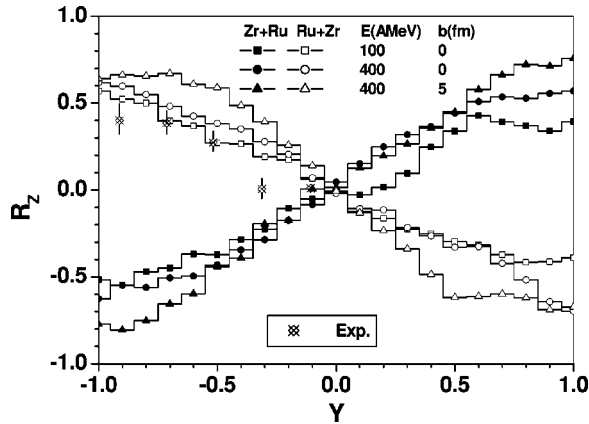


FIG. 1. The proton counting number  $R_z$  as a function of rapidity for  $^{96}\text{Ru}+^{96}\text{Ru}$ ,  $^{96}\text{Ru}+^{96}\text{Zr}$ ,  $^{96}\text{Zr}+^{96}\text{Ru}$ ,  $^{96}\text{Zr}+^{96}\text{Zr}$  at  $E=100$  A MeV  $b=0$  fm, (b),  $E=400$  A MeV,  $b=0$  fm; and (c)  $b=5$  fm, respectively. The experimental data for 400 A MeV are also given in the figure.

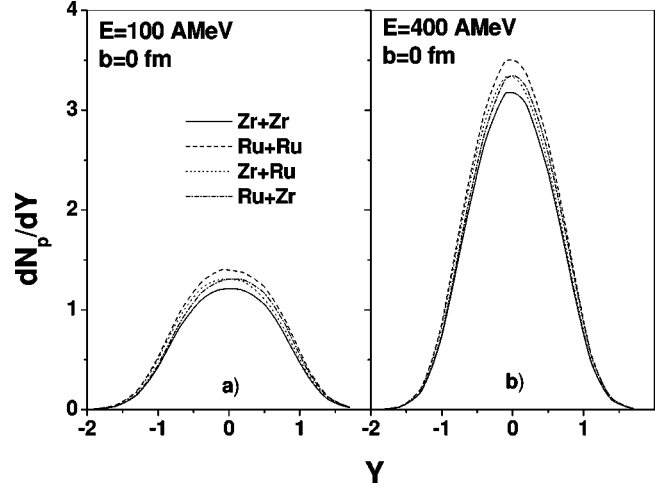


FIG. 2. The rapidity distribution of emitted protons for the same reaction as Fig. 1(a) at 100 A MeV,  $b=0$  fm and (b) at 400 A MeV,  $b=0$  fm.

target. It is obvious that if projectile and target are completely mixed then  $R_{mix}$  equals 0.5 at any rapidity and if the reaction is fully transparent, then  $R_{mix}$  should be equal to 1 at projectile rapidity and 0 at target rapidity, respectively. Figure 1 shows  $R_Z$  as a function of rapidity at beam energy 100 A MeV, impact parameter  $b=0$  fm and 400 A MeV,  $b=0$  fm and  $b=5$  fm. The experimental data (at 400 A MeV) is also given in the figure. From this figure, one can easily find that the absolute  $R_Z$  value goes from zero to about 0.5 for reactions Zr+Ru and Ru+Zr at energies 100 A MeV and 400 A MeV,  $b=0$  fm and about 0.75 for the same reactions at beam energy 400 A MeV, and  $b=5$  fm. Our calculation is in reasonable agreement with experimental data and consequently, the same conclusion concerning the nonequilibrium effect can be drawn for the 400 A MeV case. The results for  $b=0$  fm and  $b=5$  fm show that the nonequilibrium effect strongly depends on the impact parameter. However, the results of  $R_Z$  for 400 A MeV and 100 A MeV at  $b=0$  fm are indistinguishable and they lead to the same conclusion that the protons are produced in a nonequilibrium source at both 400 A MeV and 100 A MeV. It seems to us that  $R_Z$  is not very sensitive to the energy dependence of the mixing of projectile and target in the energy range studied in this work. We also find that  $R_Z$  is also not sensitive to the symmetry potential, which will be discussed in another work. In the following, we make further investigation in order to find other possible probes that may provide more clear information for the energy dependence of the degree of equilibrium.

In Figs. 2(a) and 2(b) we show the rapidity distribution of emitted protons at beam energy 100 A MeV and 400 A MeV. From Figs. 2(a) and 2(b) we can find that the reaction  $^{96}\text{Ru}+^{96}\text{Ru}$  emits more protons than does the reaction  $^{96}\text{Zr}+^{96}\text{Zr}$  because of the eight-proton difference between two reaction systems. The proton rapidity distribution for  $^{96}\text{Zr}+^{96}\text{Ru}$  and  $^{96}\text{Ru}+^{96}\text{Zr}$  is between those of Ru+Ru and Zr+Zr. Differing from the symmetric reaction Ru+Ru and Zr+Zr, the rapidity distribution of emitted protons for Ru+Zr

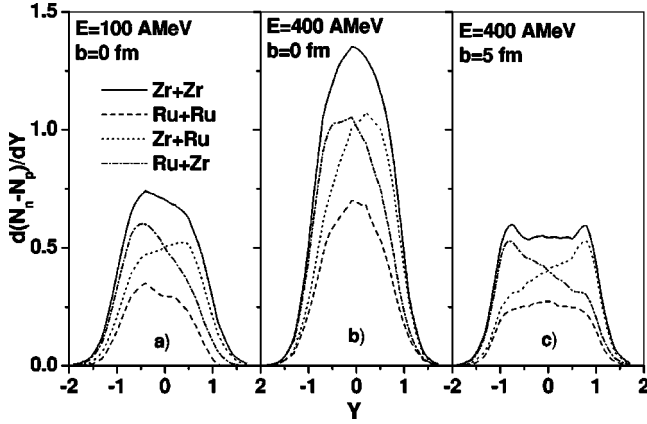


FIG. 3. The neutron-proton differential rapidity distribution for the same reactions as Fig. 1(a) at 100A MeV,  $b=0$  fm and (b) at 400A MeV,  $b=0$  fm and (c) at 400A MeV,  $b=5$  fm.

and Zr+Ru is asymmetric and the peaks deviate from  $Y=0$ . It again means that the protons are emitted from a non-equilibrium source. But again we find it difficult to give clear energy dependence of the degree of equilibrium reached. As we know that comparing with the most stable isotopes  $^{102}\text{Ru}$  and  $^{90}\text{Zr}$ ,  $^{96}\text{Ru}$  has a six-neutron deficiency and  $^{96}\text{Zr}$  has a six-neutron excess. The ratio between proton number and neutron number for  $^{96}\text{Ru}$  and  $^{96}\text{Zr}$  is 0.85 and 0.71, respectively. It would be more desirable to study the rapidity distribution of the isovector density of emitting nucleons for isospin asymmetric nuclear systems. Therefore we introduce the neutron-proton differential rapidity distribution. Figures 3(a), 3(b), and 3(c) show the neutron-proton differential rapidity distribution for  $^{96}\text{Ru}+^{96}\text{Ru}$ ,  $^{96}\text{Zr}+^{96}\text{Zr}$ ,  $^{96}\text{Zr}+^{96}\text{Ru}$ , and  $^{96}\text{Ru}+^{96}\text{Zr}$  at (a) 100A MeV,  $b=0$  fm, (b) 400A MeV,  $b=0$  fm, and (c) 400A MeV,  $b=5$  fm. First, for all three cases (a), (b), and (c), the centroids of neutron-proton differential rapidity distribution for  $^{96}\text{Ru}+^{96}\text{Zr}$  and  $^{96}\text{Zr}+^{96}\text{Ru}$  are located at the side of Zr (as target or projectile) and strongly deviate from  $Y=0$ . The centroid of distribution should be at  $Y=0$  if a system is in equilibrium. The deviation of the centroid of neutron-proton differential rapidity distribution from  $Y=0$  means there is nonequilibrium effect.

The larger the deviation from  $Y=0$  is the stronger the non-equilibrium effect is. The deviation of the centroid of neutron-proton differential rapidity distribution from  $Y=0$  for  $b=5$  fm case is much larger than that for  $b=0$  fm case. This is, of course, quite understandable. Further, one can find that the neutron-proton differential rapidity distribution of symmetric reactions  $^{96}\text{Ru}+^{96}\text{Ru}$  and  $^{96}\text{Zr}+^{96}\text{Zr}$  at 100A MeV deviates from the Gaussian shape more strongly than that at 400A MeV. It implies that there exists obvious nonequilibrium effect in the emitting nucleon process. Therefore, we can conclude that the neutron-proton differential rapidity distribution is a sensitive probe to explore the energy dependence of the degree of equilibrium for an isospin asymmetric system. We may generalize the neutron-proton differential rapidity distribution by introducing  $t^{-3}\text{He}$  differential rapidity distribution to probe equilibration in isospin asymmetric colliding systems.

However, emitted single nucleons can only characterize a limited part of the system, therefore we further study the isospin distribution in LCP and IMF in addition to nucleons. In Figs. 4(I) and 4(II), we show the average  $N/Z$  ratios in emission of nucleons, LCP and IMF at projectile (a), central (b), and target (c) rapidity region in four systems at 400A MeV and 100A MeV,  $b=0$  fm, respectively. The projectile rapidity region is defined by  $1.5 \geq Y \geq 0.5$ , the target rapidity region by  $-0.5 \geq Y \geq -1.5$ , and the central rapidity region by  $0.5 \geq Y \geq -0.5$ . The figures first tell us about a basic feature that the difference between the average  $N/Z$  ratios of emitted nucleons of four colliding systems with different isospin asymmetry is much greater than that between the average ratios of LCP and IMF of four systems at three rapidity regions, i.e., the more neutron (proton)-rich systems emit more neutrons (protons) while the average  $N/Z$  ratios of LCP and IMF for these four systems are relatively close. This behavior is stronger at 100A MeV case. The experimental measurements at tens of A MeV energy region [10] found that the more asymmetric the system is, the stronger the system will be breaking up into still more neutron-rich (-deficient) light fragments while the  $N/Z$  ratio of heavier fragments remains relatively insensitive. Our calculation results show similar tendency, only because of the en-

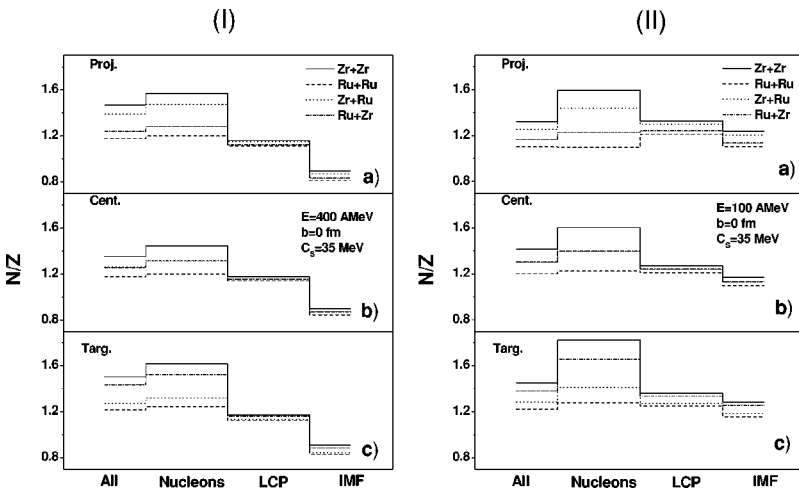


FIG. 4. (I) The average  $N/Z$  ratio of emitted nucleons, light charged particles, and intermediate mass fragments at (a) projectile rapidity region, (b) central rapidity region, and (c) target rapidity region for the same reactions as Fig. 1 at  $E=400$ A MeV,  $b=0$  fm. (II) The same as (I) but at  $E=100$ A MeV.

ergy difference, here the  $N/Z$  ratios of emitted nucleons, LCP, and IMF are compared instead of comparing the  $N/Z$  ratios for LCP and IMF in Ref. [10] where the energy was relatively low. The second feature is that the average  $N/Z$  ratio of emitted nucleons generally is the largest, and then, that of LCP and the  $N/Z$  ratio of IMF is the smallest in all rapidity regions, which implies that the single nucleons are more neutron rich and LCP and IMF are more isospin symmetric.

It is more meaningful to investigate whether the  $N/Z$  ratio of IMF for mixing reaction converges or not as far as the degree of equilibrium is concerned because IMF is produced at late stage of reaction [11]. When we attend to the  $N/Z$  ratios at target and projectile rapidity regions, we find that not only the  $N/Z$  ratios of emitted nucleons for the two mixing reactions  $^{96}\text{Zr}+^{96}\text{Ru}$  and  $^{96}\text{Ru}+^{96}\text{Zr}$  but also those of LCP and IMF do not match each other but they are closer to Zr+Zr or Ru+Ru at respective rapidity region. It means that not only the nucleons but also the IMF are not emitted from a completely equilibrium source. Of course, the difference of the average  $N/Z$  ratio of IMF for reactions Zr+Ru and Ru+Zr is weaker than emitted nucleons, which is understandable because IMF is produced at a later stage. One can further find that the difference of the  $N/Z$  of IMF for Zr+Ru and Ru+Zr at 100A MeV is greater than that at 400A MeV. It may also imply the energy dependence of the degree of equilibrium with respect to the isospin degree of freedom. The energy dependence of the degree of equilibrium is because the two-body collisions become more violent as energy increases from 100A MeV to 400A MeV.

By comparing Figs. 4(I) and 4(II), one can find that the  $N/Z$  ratio decreases as energy increases from 100A MeV to 400A MeV for all four systems. It would be interesting to study the reason of this behavior. In Fig. 5 we show the yields of the isotopes of the most abundant IMF charges, (a) Li, (b) Be, and (c) B for Zr+Zr, Zr+Ru, Ru+Zr, and Ru+Ru at 100A MeV and Zr+Zr and Ru+Ru at 400A MeV, respectively. One can easily find that the yields of isotopes of Li, Be, and B for 100A MeV case are about several times greater (for non-neutron-rich isotopes) to several tens of times greater (for neutron-rich isotopes) than those for 400A MeV case. The curves for isotope distribution of Li, Be, and B for 100A MeV are flatter than those for 400A MeV and furthermore the most abundant isotopes of Li, Be, and B are always those of most stable ones for 100A MeV case while they are always those of the lightest isotopes for 400A MeV case. Consequently, the average  $N/Z$  of IMF is reduced as energy increases from 100A MeV to 400A MeV. Another obvious difference between the isotope distribution of Li, Be, and B for 100A MeV and 400A MeV cases is the dependence of the yields of the neutron-rich (-deficient) isotopes on the initial system. For 100A MeV case, the relative yields of the neutron-rich (-deficient) isotopes depends on the  $N/Z$  ratio of the initial system. The initial system with larger  $N/Z$  ratio produces more neutron-rich isotopes and vice versa. We notice that for this case (100A MeV), the curves of the isotope distribution of Li, Be, and B in mixing reactions Zr+Ru and Ru+Zr do not merge into one curve but they are close to those of respective reac-

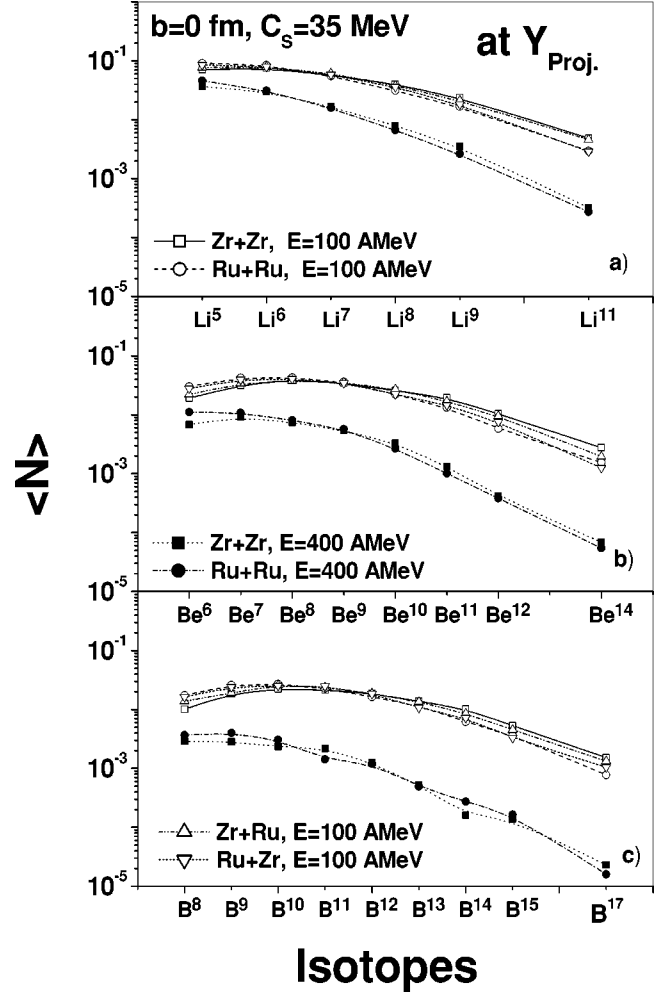


FIG. 5. The isotope distribution of Li, Be, and B at projectile region for the same reactions as Fig. 1 at  $E=100$  A MeV and 400A MeV,  $b=0$  fm, respectively.

tions Zr+Zr or Ru+Ru with the same projectile. It means that there exist certain memory effects at 100A MeV case. For 400A MeV case, this memory effect appearing in the isotope distribution of IMF charges disappears.

In summary, we have studied the isospin relevant probes; normalized proton counting  $R_Z$ , the proton rapidity distribution, the neutron-proton differential rapidity distribution as well as the  $N/Z$  ratio of single nucleons, LCP, IMF at central, projectile, and target rapidity regions for four 96 mass systems  $^{96}\text{Ru}+^{96}\text{Ru}$ ,  $^{96}\text{Ru}+^{96}\text{Zr}$ ,  $^{96}\text{Zr}+^{96}\text{Ru}$ , and  $^{96}\text{Zr}+^{96}\text{Zr}$  at 100A MeV and 400A MeV with isospin-dependent QMD. All these probes concerning the single nucleon emission studied in this work show that the emitted nucleons are not from an equilibrium source and there exists an obvious non-equilibrium effect. We propose that the neutron-proton differential rapidity distribution is a sensitive probe to the energy dependence of the degree of equilibrium in single nucleon emission in intermediate-energy heavy-ion collisions. The average  $N/Z$  ratios of IMF in mixing reactions  $^{96}\text{Ru}+^{96}\text{Zr}$  and  $^{96}\text{Zr}+^{96}\text{Ru}$  with the same  $N/Z$  and mass do not converge but they are closer to Zr+Zr or Ru+Ru at respective rapidity region. The difference of  $N/Z$  ratios of

IMF between  $^{96}\text{Ru}+^{96}\text{Zr}$  and  $^{96}\text{Zr}+^{96}\text{Ru}$  at 100A MeV is larger than that at 400A MeV, which shows the energy dependence of the nonequilibrium effect with respect to isospin degree of freedom. Furthermore, we find the average  $N/Z$  ratios of IMF at projectile and target rapidity regions of IMF decreases considerably as energy increases from 100A MeV to 400A MeV, which may result from the change of the behavior of the isotope distribution of IMF charge from 100A MeV to 400A MeV. The analyzing of isotope distribu-

tion of IMF charges at projectile rapidity region for four 96 mass systems shows existence of memory effect at 100A MeV but not at 400A MeV concerning isospin degree of freedom.

Supported by National Natural Science Foundation of China under Grant No. 19975073 and Science Foundation of Nuclear Industry and the Major State Basic Research Development Program under Contract No. G20000774

- 
- [1] R. Nebauer and J. Aichelin, Nucl. Phys. **A681**, 353 (2001).  
[2] J.P. Bondorf, A.S. Botvina, A.S. Iljinov, I.N. Mishustin, and K. Sneppen, Phys. Rep. **257**, 133 (1995).  
[3] D.H.E. Gross and K. Sneppen, Nucl. Phys. **A567**, 417 (1993).  
[4] J. Aichelin, Phys. Rep. **202**, 233 (1991), and references therein.  
[5] P.B. Gossiaux, R. Puri, C. Hartnack, and J. Aichelin, Nucl. Phys. **A619**, 379 (1997).  
[6] F. Rami *et al.*, Phys. Rev. Lett. **84**, 1120 (2000).  
[7] W. Reisdorf, FOPI Collaboration, in *Multifragmentation*, edited by H. Fedmeier, J. Knoll, W. Nörenberg, and J. Wambach (GSI, Darmstadt, 1999).  
[8] C. Hartnack *et al.*, Nucl. Phys. **A495**, 303 (1989).  
[9] Fan Sheng, Li Zhuxia, Zhao Zhixiang, and Ding Dazhao, Eur. Phys. J. A **4**, 61 (1999).  
[10] S.J. Yennello *et al.*, Nucl. Phys. **A681**, 317c (2001).  
[11] J.P. Bondorf, A.S. Botvina, I.N. Mishustin, and S.R. Souza, Phys. Rev. Lett. **73**, 628 (1994).